FULL PAPER

BJC

British Journal of Cancer (2013) 109, 2587–2596 | doi: 10.1038/bjc.2013.642

Keywords: natural compounds; stem cells; growth arrest; EMT; pro-survival signaling

Silencing NOTCH signaling causes growth arrest in both breast cancer stem cells and breast cancer cells

S Suman[1], TP Das[1] and C Damodaran*[,1]

[1]Department of Biomedical Sciences, Paul L Foster School of Medicine, Texas Tech University Health Sciences Center, El Paso, TX, USA

Background: Breast cancer stem cells (BCSCs) are characterized by high aldehyde dehydrogenase (ALDH) enzyme activity and are refractory to current treatment modalities, show a higher risk for metastasis, and influence the epithelial to mesenchymal transition (EMT), leading to a shorter time to recurrence and death. In this study, we focused on examination of the mechanism of action of a small herbal molecule, psoralidin (Pso) that has been shown to effectively suppress the growth of BSCSs and breast cancer cells (BCCs), in breast cancer (BC) models.

Methods: $ALDH^-$ and $ALDH^+$ BCCs were isolated from MDA-MB-231 cells, and the anticancer effects of Pso were measured using cell viability, apoptosis, colony formation, invasion, migration, mammosphere formation, immunofluorescence, and western blot analysis.

Results: Psoralidin significantly downregulated NOTCH1 signaling, and this downregulation resulted in growth inhibition and induction of apoptosis in both $ALDH^-$ and $ALDH^+$ cells. Molecularly, Pso inhibited NOTCH1 signaling, which facilitated inhibition of EMT markers (β-catenin and vimentin) and upregulated E-cadherin expression, resulting in reduced migration and invasion of both $ALDH^-$ and $ALDH^+$ cells.

Conclusion: Together, our results suggest that inhibition of NOTCH1 by Pso resulted in growth arrest and inhibition of EMT in BCSCs and BCCs. Psoralidin appears to be a novel agent that targets both BCSCs and BCCs.

Regardless of early diagnosis and advances in treatment, metastatic breast cancer (BC) remains a leading cause of cancer-related death among women (Stockler *et al*, 2000; Gangopadhyay *et al*, 2013). Recent evidence indicates that cancer stem cells (CSCs) govern enhanced tumorigenicity and capacity for self-renewal/differentiation in various cancers (breast, brain, prostate, colon, pancreatic, head and neck, melanoma, and multiple myeloma) (Dontu *et al*, 2004; Visvader and Lindeman, 2008). In addition, CSCs are responsible for tumour initiation, progression, metastasis, and relapse (Velasco-Velazquez *et al*, 2011; Tsang *et al*, 2012).

Breast cancer stem cells (BCSCs), which were first isolated on the basis of cell surface marker expression, are characterized as $ESA^+/CD44^+/CD24^-$ cells that lack the expression of the lineage markers CD2, CD3, CD10, CD 16, CD18, CD31, CD64, and CD140b (Lin^-), and these cells exhibit a potent *in vivo* tumorigenicity in immunodeficient mice (Al-Hajj *et al*, 2003). Ginestier *et al* (2007) isolated BCSCs based on a functional marker, aldehyde dehydrogenase (ALDH) enzyme, using the aldeflour assay, and this enzyme has been shown to be associated with the 'stemness' characteristics of CSCs. The wide variety of biological processes that are regulated by CSCs includes cell proliferation, self-renewal *vs* differentiation, and stem cell self-protection throughout the lifespan of the organism (Ginestier *et al*, 2007; Croker and Allan, 2012; Velasco-Velazquez *et al*, 2012). Aldehyde dehydrogenase activity appears to be a reliable universal hallmark of BCSCs and is associated with metastasis, poor prognosis, and

*Correspondence: Dr C Damodaran; E-mail: C.damodaran@ttuhsc.edu

Received 5 August 2013; revised 19 September 2013; accepted 24 September 2013; published online 15 October 2013

clinical outcome in BC patients (Ginestier *et al*, 2007; Charafe-Jauffret *et al*, 2009, 2010; Marcato *et al*, 2011a; Yoshioka *et al*, 2011).

Breast cancer stem cells with enhanced ALDH activity are linked to many signaling pathways that regulate the epithelial to mesenchymal transition (EMT) characteristics, such as invasiveness and metastasis (Giordano *et al*, 2012; Smalley *et al*, 2012). Among these pathways, the NOTCH pathway is associated with the regulation of cell fate at several distinct developmental stages of the mammary gland and has been implicated in cancer initiation and progression (Dontu *et al*, 2004; Shi and Harris, 2006; Gangopadhyay *et al*, 2013). In mammals, the NOTCH signaling pathway involves four NOTCH receptors (NOTCH1, 2, 3, and 4) and five ligands (Delta-like-1 or DLL-1, 3, 4 and Jagged1 and 2) (Andersen *et al*, 2012). NOTCH signaling is activated by direct cell–cell contact involving ligand-receptor binding, which is followed by proteolytic cleavage of the intracellular domain of NOTCH (NICD), yielding the active form of the NOTCH receptor. The NICD cleavage products subsequently translocate to the nucleus and interact with the transcription complex to activate downstream events such as expression of the HES/HEY family of genes involved in repression of tissue-specific transcription factors (Miele, 2006). NOTCH signaling is implicated in embryogenesis and BC tumorigenesis potentially by maintaining BCSCs via influence on the EMT (Smalley *et al*, 2012). The EMT proceeds via a complex molecular and cellular program that involves the loss of epithelial markers, such as E-cadherin, and acquisition of mesenchymal markers, such as vimentin. Epithelial cells undergo loss of cell–cell adhesion and planar and apical-basal polarity and acquire mesenchymal phenotypes with respect to motility and invasiveness, leading to metastasis and resistance to apoptosis and chemotherapy (Thiery *et al*, 2009). At the molecular level, the important drivers of EMT include Snail, Zeb1, Twist, and KLF8 (Thiery *et al*, 2009).

In the current study, we explored the potential of the herbal bioactive compound psoralidin (Pso; 3, 9-dihydroxy-2-prenylcoumestan) for targeting NOTCH1-induced EMT in BC cells (breast cancer cell, BCCs) and BCSCs. Psoralidin, which was derived from the seeds of the Asian medicinal plant *Psoralea corylifolia,* exhibits a variety of biological activities, such as antioxidant, antibacterial, antidepressant, anticoagulant, anti-inflammatory, antiallergic, ROS modulatory, and anticancer activities (Vadodkar *et al*, 2012; Das *et al*, 2013; Gulappa *et al*, 2013); however, the anticancer effects of Pso on CSCs and especially on BCSCs have yet to be established. Overall, the results from our study suggest that Pso inhibits NOTCH1 signaling in both BC cells and BCSCs and results in the inhibition of growth and EMT, suggesting that Pso may serve as a potential therapeutic agent for the prevention and cure of BC.

MATERIALS AND METHODS

Cell lines and reagents. Human mammary immortalized cells (MCF-12A) and the BC epithelial cell line MDA-MB-231 were purchased from the American Type Culture Collection (Manassas, VA, USA). MCF-12A cells were maintained in 1 : 1 mixture of Dulbecco's modified Eagle's medium (DMEM) and Ham's F12 medium with 20 ng ml^{-1} human epidermal growth factor, 100 ng ml^{-1} cholera toxin, 0.01 mg ml^{-1} bovine insulin, 500 ng ml^{-1} hydrocortisone, and 5% horse serum. MDA-MB-231 cells were grown in DMEM containing L-glutamine and sodium pyruvate, supplemented with 10% fetal bovine serum and 1% antibiotic and antimycotic solution in a humidified atmosphere of 5% CO_2 at 37 °C in an incubator. Human BCSCs were purchased from Celprogen (San Pedro, CA, USA) and maintained in human BCSC expansion and undifferentiation media. ALDH$^+$ cells were also expanded and maintained in stem cell expansion and undifferentiation media. Psoralidin was purchased from Santa Cruz Biotechnology (Dallas, TX, USA).

Aldefluor assay for separation of the ALDH$^+$ population by flow cytometry. The ALDEFLUOR kit for ALDH-based cell detection (StemCell Technologies, Durham, NC, USA) was used to identify and isolate the cell population with high ALDH enzyme activity from MDA-MB-231 BCCs according to the manufacturer's instructions. Approximately, 1×10^6 cells were suspended in 1 ml ALDEFLUOR assay buffer containing 5 μl of activated ALDEFLOUR reagent (BAAA; BODIPY aminoacetaldehyde) and incubated for 45 min at 37 °C. As a negative control, an aliquot of cells was treated with the specific ALDH inhibitor diethylaminobenzaldehyde (DEAB). Following incubation, cells were centrifuged, and the cell pellets were resuspended in 0.5 ml ALDEFLOUR assay buffer and maintained on ice until sorting. Aldehyde dehydrogenase activity was measured on the basis of the amount of fluorescent reaction product produced. Cells with high ALDH activity were labeled as ALDH$^+$, and cells with no ALDH activity were labeled as ALDH$^-$.

Cell viability. Cells were treated with various concentrations of Pso, doxorubicin, docetaxel, 5-FU, and DMSO (vehicle) for 24 h. Cell viability was quantified using the trypan blue exclusion method or 3-(4, 5-dimethylthiazol-2-yl)-2, 5-diphenyltetrazolium-bromide (MTT) assay as described previously (Srinivasan *et al*, 2007, 2009).

Apoptosis assay. Quantification of apoptosis was performed with the Annexin V-FITC apoptosis kit (BD Pharmingen, San Diego, CA, USA). Cells were treated with the respective Pso IC_{50} values. Cells were harvested 24 h after treatment and suspended in 500 μl of binding buffer. Cells were then stained with 5 μl of FITC-Annexin-V and 5 μl of propidium iodide for 15 min in the dark at room temperature and then analyzed by flow cytometer (BD Accuri C6 flow cytometer, San Jose, CA, USA).

Mammosphere formation assay. Different methods were used to assess the mammosphere formation ability of ALDH$^-$ cells and ALDH$^+$ cells. Single-cell suspensions were made and cultured at a density of 4000 cells per 2 ml in DMEM containing 10% FBS. The same number of cells was cultured in MammoCult basal medium containing MammoCult proliferation supplements, 4 μg ml^{-1} of heparin, and 0.48 μg ml^{-1} of hydrocortisone (StemCell Technologies) in ultra-low attachment plates (Corning, Acton, MA, USA). A mammosphere assay was also performed in DMEM/F-12 media containing 5 mg ml^{-1} insulin, 0.5 mg ml^{-1} hydrocortisone, 2% B27, and 20 ng ml^{-1} epidermal growth factor, and cells were seeded into six-well ultra-low attachment plates. Simultaneously, single-cell suspension cultures were treated with Pso at its IC_{50} value, and both control and treated cells were allowed to grow for 2–3 weeks to form mammospheres, which were then counted.

Soft agar colony formation assay. A colony formation assay was performed to monitor anchorage-independent growth using CytoSelect 96-well *In Vitro* Tumor Sensitivity Assay kit (Cell Biolabs Inc, San Diego, CA, USA). ALDH$^-$ and ALDH$^+$ cells (5×10^3) were harvested and assayed as described (Suman *et al*, 2013). Cells were treated with Pso at the IC_{50} value, and colonies were stained with 0.005% crystal violet 10 days after seeding and were counted manually under an inverted phase-contrast microscope.

Invasion assay. Invasion assays were performed and evaluated using Boyden chambers equipped with polyethylene terephthalate membranes with 8-μm pores (BD Biosciences, San Jose, CA, USA) as described previously (Das *et al*, 2013). Matrigel that contained extracellular matrix proteins was layered on top of the transwell plate membrane. Cells were cultured in complete medium for 24 h

before detachment with trypsin-EDTA. Subsequently, 1×10^5 cells per chamber were resuspended in culture medium. Cells were allowed to migrate towards the lower chamber for 24 h. The upper transwell was removed, and the cells that remained in the upper chamber were removed with a cotton swab. The membrane was stained with crystal violet. Invasive cells were counted using an AMG-EVOS digital inverted microscope.

Wound healing migration assay. $ALDH^-$ and $ALDH^+$ cells and BCSCs were cultured in six-well plates until they reached 100% confluency. A linear wound was gently created in monolayers with a sterile pipette tip. The cells were then washed with growth medium to remove the detached cells, and the medium was replenished with fresh medium (Das *et al*, 2013). The cell culture plates were transferred to a Biostation CT (Nikon Instruments Inc, Melville, NY, USA) programmed to take photographs every 2 h for up to 36 h. The photographs at different time points were aligned using the NIS-Element AR software, and the distance between the opposing edges of the wound was measured in micrometers.

Protein extraction and western blotting. $ALDH^-$ and $ALDH^+$ cells were seeded in six-well plates. Following 24 h of synchronization, cells were treated with Pso IC_{50} value or DMSO (vehicle). Cells were harvested after 12 and 24 h of treatment. Whole-cell lysates were prepared with Mammalian protein extraction reagent (Thermo Scientific, Rockford, IL, USA) according to the manufacturer's protocol. Western blotting was performed using specific antibodies against NOTCH1 (Sigma, St Louis, MO, USA), HES-1, HRT-1, nuclear factor NFκB (p65), BCL-2, vimentin (Santa Cruz Biotechnologies, Dallas, TX, USA) β-catenin, E-cadherin, twist and Slug (Cell Signaling, Danvers, MA, USA). Positive bands were detected with the enhanced chemiluminescence method.

Immunofluorescence staining. Immunofluorescence assays were performed as described earlier (Das *et al*, 2013; Gulappa *et al*, 2013), briefly, BCSCs and BCCs were plated on glass coverslips and treated with respective IC_{50} dose of Pso for 24 h. After fixation, the cells were then incubated for 2 h with antibodies against E-cadherin and β-catenin followed by incubation for 2 h with respective secondary antibodies. Coverslips were washed with PBS thoroughly followed by mounting using Antifade with DAPI mountant, and observed and photographed using a Nikon Eclipse Ti confocal microscope.

Small interfering RNA transfection. $ALDH^-$ and $ALDH^+$ cells were seeded in six-well plates at a density of 2×10^5 cells per well, and after 24 h of synchronization, the cells were transiently transfected with 20 nM siRNA (siNOTCH1) as well as control siRNA using TransIT-siQUEST transfection reagent (Mirus, Madison, WI, USA). Transfected cells were harvested after 24 h, and cell proliferation was measured using the trypan blue exclusion method. Whole-cell lysates were prepared for western blot analysis as described above.

Statistical analysis. Statistical analyses were performed using GraphPad prism 6.0a software (GraphPad Software Inc, La Jolla, CA, USA). The results are given as mean ± s.e.m. Analysis was performed using a two-tailed unpaired, Student's *t*-test. Differences were considered statistically significant with $P \leqslant 0.05$.

RESULTS

Characterization of BCCs and BCSCs. We examined BCCs ($ALDH^-$) and BCSCs ($ALDH^+$) that were sorted from MDA-MB-231 cells. In the BCC line, MDA-MB-231, the $ALDH^+$ population represented less than 1.9% of the cells (Figure 1A). In addition, we used commercially available BCSCs (Celprogen) and normal breast epithelial cells in our experiments. First, we analyzed $ALDH^-$ and $ALDH^+$ cell proliferation. A 1.58-fold increase in cell proliferation of $ALDH^+$ cells was noted as compared with $ALDH^-$ cells (Figure 1B). Similarly, $ALDH^+$ cells showed a five-fold increase in colony formation as compared with $ALDH^-$ cells (Figure 1C). Next, we determined the mammosphere-forming capability of $ALDH^-$ and $ALDH^+$ cells. Mammospheres are floating colonies formed by a single cell in anchorage-independent cell cultures, and this assay is used to identify mammary stem cells (Ponti *et al*, 2005; Grimshaw *et al*, 2008). $ALDH^-$ and $ALDH^+$ cells were allowed to grow for 15 days on ultra-low binding plates. The $ALDH^+$ cells generated 2.5-fold (69 ± 8.48) more mammospheres than $ALDH^-$ (27.5 ± 3.53) cells (Figure 1D). The migration assays revealed that $ALDH^+$ cells migrated towards the wound space 92.99% more rapidly than $ALDH^-$ (50.51%), and BCSCs (72.55%) (Figure 1E). Similarly, increased invaded cells were seen in $ALDH^+$ (2.15) and BCSCs (2.0-fold) as compared with the $ALDH^-$ cells (Figure 1F).

Breast cancer stem cells ($ALDH^+$ and commercial BCSCs) showed resistance to chemotherapeutic drugs. Breast cancer stem cells are known to be resistant to chemotherapy; thus, we tested whether chemotherapeutic agents such as doxorubicin (0.5, 1, and 2.5 μM, Figure 2A), docetaxel (1, 10, and 100 μM, Figure 2B), and 5-FU (1, 10, and 20 μM, Figure 2C) inhibit the growth of $ALDH^-$ and $ALDH^+$ cells. Interestingly, doxorubicin and docetaxel significantly sensitized both $ALDH^-$ and $ALDH^+$ cells; however, $ALDH^-$ cells were more sensitive to these agents than the $ALDH^+$ cells and commercial BCSCs (Figure 2A and B). All cells tested ($ALDH^-$, $ALDH^+$, and commercial BCSC) were less sensitive to 5-FU ($P < 0.05$) (Figure 2C).

Psoralidin inhibits cell viability and mammosphere formation and induces apoptosis in both BCCs and BCSCs. Having established the aggressive growth of BSCSs and the resistance of these cells to chemotherapeutic agents in the experiments described above, we explored whether Pso suppresses the growth of BSCS. $ALDH^-$ cells, $ALDH^+$ cells, commercial BCSCs, and normal mammary epithelial cells (MCF-12A) were treated with 10, 15, 20, and 25 μM of Pso or vehicle (DMSO) for 24 h and then examined for cell viability. All three BCC populations ($ALDH^-$ cells, $ALDH^+$ cells, and commercial BSCSs) were sensitive to Pso treatment with IC_{50} values ranging from 18 to 21 μM (Figure 3A); however, the MCF-12A cells were resistant to Pso. To confirm these results, we performed colony formation assays with $ALDH^-$ and $ALDH^+$ cells in the presence of their respective Pso IC_{50} concentrations or an equal volume of vehicle. Psoralidin treatment significantly inhibited the colony formation ability of both $ALDH^-$ and $ALDH^+$ cells ($P < 0.05$; Figure 3B). In addition, for mammosphere analysis, $ALDH^-$ and $ALDH^+$ cells were treated with the Pso IC_{50} dose or the appropriate volume of vehicle. Treatment of Pso significantly inhibited mammosphere formation ($P < 0.05$), and the size of the mammospheres was dramatically reduced in $ALDH^-$ and $ALDH^+$ cells (Figure 3C). Furthermore, we determined whether Pso induces apoptosis in $ALDH^-$ cells, $ALDH^+$ cells, and commercial BSCSs. No significant induction of apoptosis was observed for any of the three cell types following treatment with Pso at 20 μM, although a higher concentration of Pso (30 μM) resulted in a significant induction of apoptosis for all three cell types. Specifically, 53.60%, 44.1%, and 45.9% of cells were apoptotic in samples of $ALDH^-$ cells, $ALDH^+$ cells, and commercial BCSCs, respectively (Figure 3D).

Psoralidin inhibits NOTCH1 signaling in both $ALDH^-$ and $ALDH^+$ cells. NOTCH signaling is implicated in the development and maintenance of BCSCs and thus can drive tumorigenisis (Grudzien *et al*, 2010). $ALDH^-$ and $ALDH^+$ cells were treated with vehicle or IC_{50} concentrations of Pso. $ALDH^+$ cells showed high expression of NOTCH1 compared with

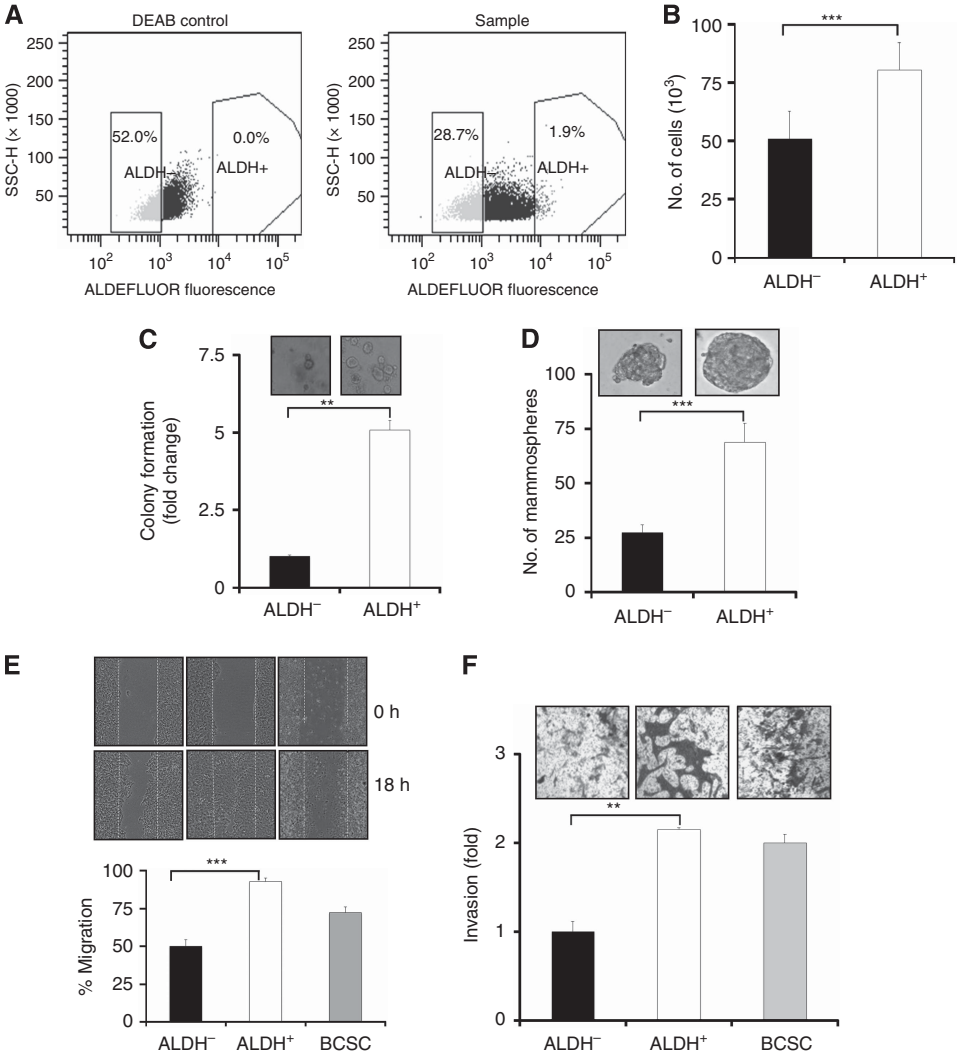

Figure 1. Breast cancer stem cells exhibit aggressive growth and resistance to chemotherapeutic agents: (**A**) Aldefluor assay showing the percentage of ALDH$^-$ and ALDH$^+$ cells population in MDA-MB-231 cells by flow cytometry analysis. (**B**) To check cell proliferation, ALDH$^-$ and ALDH$^+$ 25×10^3 cells were plated in 24-well plates and allowed to grow for 24 h followed by harvesting and counting of viable cells using a trypan blue exclusion assay. (**C**) To assess anchorage-independent growth, 5×10^3 cells (ALDH$^-$ and ALDH$^+$ cells) were grown in soft agar for 10 days. Colonies were stained with crystal violet and counted manually. (**D**) A mammosphere assay was performed using 4×10^3 cells 2 ml^{-1} of DMEM/Mammocult media in ultra-low attachment plates. The cells were allowed to grow for 2 weeks, and then mammospheres were counted. (**E**) ALDH$^-$, ALDH$^+$, and commercial BCSCs were plated in six-well plates and grown until confluent. A uniform wound was created in the center of the monolayer. The wound gap was photographed in a Biostation CT programmed to take pictures every 2 h. The distance between the edges of wound was measured in μM using NIS-Element software, and statistical analysis was performed. (**F**) A transwell invasion assay was performed with ALDH$^-$ cells, ALDH$^+$ cells, and commercial BCSCs using Boyden chambers. The invasive cells were stained with crystal violet and counted. Data are expressed as mean ± s.e.m. of two independent experiments. Student's *t*-test was used to calculate statistical significance. *$P<0.05$, **$P<0.005$, and ***$P<0.0001$.

ALDH$^-$ cells, and Pso treatment downregulated NOTCH1 expression in both ALDH$^-$ and ALDH$^+$ cells (Figure 4A). To determine whether NOTCH1 downstream events are inhibited by Pso, we examined the expression of one of the important NOTCH1 target genes, HES1 (Iso *et al*, 2003). Indeed, high expression of HES1 was observed in ALDH$^+$ cells, and Pso treatment diminished HES1 levels in both ALDH$^-$ and ALDH$^+$ cells (Figure 4A).

Previous reports demonstrated that BCSCs show increased motility and invasion and therefore promote metastasis (Velasco-Velazquez *et al*, 2012). Thus, we analyzed the expression of some of the important EMT marker genes in BCCs and BCSCs by western blot analysis. Interestingly, E-cadherin was expressed at lower levels in ALDH$^+$ cells than in ALDH$^-$ cells, and the treatment of these cells with Pso resulted in increased expression of E-cadherin at both the 12- and 24-h time points in ALDH$^-$ and ALDH$^+$ cells (Figure 4B). On the other hand, Pso treatment of ALDH$^-$ and ALDH$^+$ cells resulted in decreased levels of β-catenin and vimentin at the 24-h time point (Figure 4B). Similar results were observed using immunofluorescence; Pso-treated ALDH$^-$ and ALDH$^+$ cells exhibited increased E-cadherin expression (Figure 4C) and decreased β-catenin levels (Figure 4D).

Psoralidin inhibits migration and invasion of BC and BCSCs. After confirming a downregulation of EMT markers in Pso-treated ALDH$^-$ and ALDH$^+$ cells, we performed phenotypic analysis to examine migration and invasion in both cell types. In a wound healing migration assay, vehicle-treated ALDH$^+$ cells exhibited

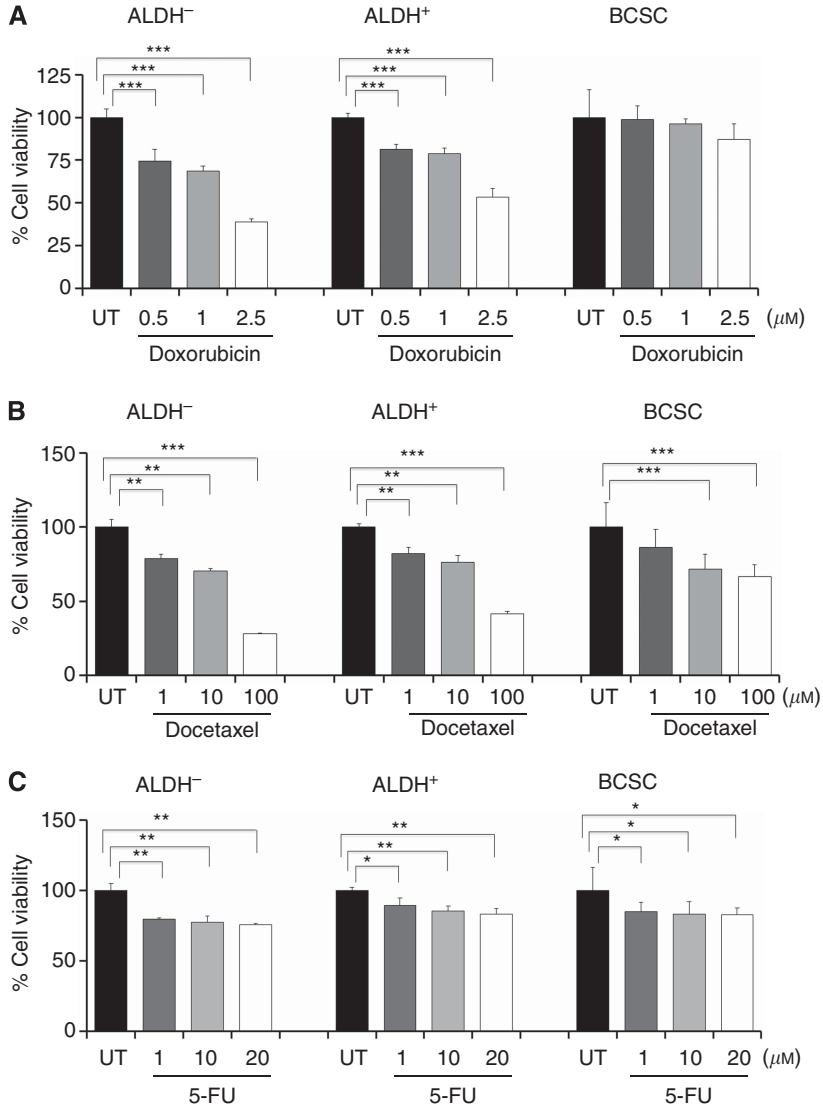

Figure 2. Breast cancer stem cells show resistance to chemotherapeutic agents. (**A**–**C**) ALDH$^-$ and ALDH$^+$ cells were exposed to different concentrations of chemotherapeutic agents (doxorubicin, docetaxel, or 5-FU) for 24 h. Cell viability was measured by MTT assay. Data are expressed as mean ± s.e.m. of three independent experiments. Student's *t*-test was used to calculate statistical significance. *$P<0.05$, **$P<0.005$, and ***$P<0.0001$.

complete wound recovery after 18 h, whereas vehicle-treated ALDH$^-$ cells lagged behind at the 18 h time point (Figure 5A). In contrast, Pso treatment of these cells significantly inhibited the migration of ALDH$^-$ cells to 29.4% and of ALDH$^+$ cells to 19.77% and in BCSCs to 82% as compared with the vehicle-treated counterparts (Figure 5A). Furthermore, we performed a transwell invasion assay and demonstrated that ALDH$^+$ cell invasion increased by 1.79-fold and commercial BCSC invasion increased by 1.7-fold as compared with the ALDH$^-$ cells. Psoralidin treatment of these cells induced a significant inhibition of ALDH$^-$ cell invasion (0.65-fold, $P<0.05$), ALDH$^+$ cell invasion (0.30-fold, $P\leqslant0.0005$), and commercial BCSC invasion (0.46-fold, $P=0.0086$) when compared with the respective vehicle-treated counterparts (Figure 5B).

Psoralidin inhibits pro-survival genes and simultaneously induces pro-apoptotic genes in BCCs and BCSCs. The NFκB transcription factor is an important regulator of genes that control cell proliferation and cell survival. Accumulating evidence indicates an important role for NFκB in BC (Mao *et al*, 2013) and various natural products have been shown to inhibit NFκB activity and hence inhibit the proliferation of tumour cells (Wang *et al*, 2006). As a result, we tested the effects of Pso on NFκB (p65) expression and the downstream targets of this transcription factor. Interestingly, NFκB expression was inhibited by Pso in both ALDH$^-$ and ALDH$^+$ cells (Figure 6A). A significant decrease in the expression of the downstream antiapoptotic protein BCL-2 was also observed along with a concurrent increase in the expression of the pro-apoptotic BAX protein (Figure 6A). Finally, examination of the expression of caspase cascade proteins revealed induction of the proteolytically cleaved caspase-3, caspase-9, and poly-ADP ribose polymerase (PARP) following Pso treatment, indicating that Pso mediates apoptosis in ALDH$^-$ and ALDH$^+$ cells (Figure 6B).

NOTCH1 silencing inhibits cell proliferation and EMT in ALDH$^-$ and ALDH$^+$ cells. To determine whether inhibition of NOTCH1 expression is responsible for the downregulation of EMT and growth arrest in ALDH$^-$ and ALDH$^+$ cells, we transfected NOTCH1 siRNA (siNOTCH1) or the control scrambled siRNA into ALDH$^-$ and ALDH$^+$ cells and examined cell viability and EMT marker expression. The number of viable cells was decreased by more than 50% in siNOTCH1-transfected both ALDH$^-$ and

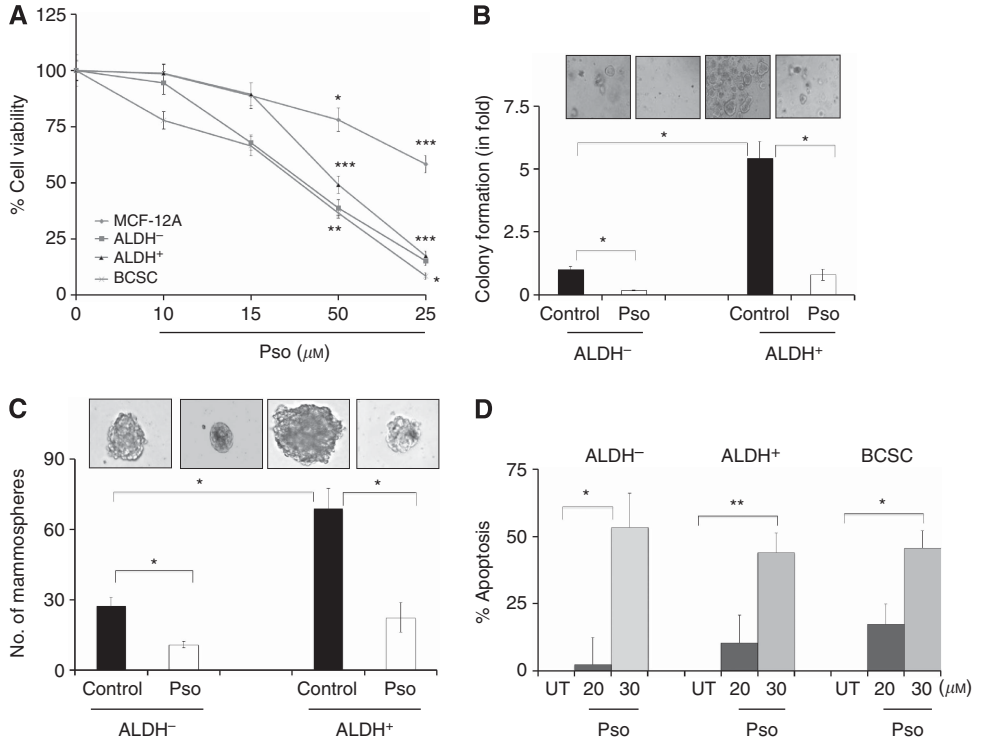

Figure 3. Psoralidin inhibits cell growth, mammosphere formation and induces apoptosis in BC and BCSCs. (**A**) ALDH$^-$ cells, ALDH$^+$ cells, commercial BCSCs, and normal breast epithelial cells (MCF-12A) were treated with vehicle (DMSO) or the indicated dose of Pso for 24 h. Cell viability was determined using a trypan blue exclusion assay. Data are expressed as mean ± s.e.m. of two independent experiments done in triplicates. (**B**) Anchorage-independent growth of ALDH$^-$ and ALDH$^+$ cells was determined by assessing the colony-forming ability of these cells. Approximately, 5×10^3 cells were treated with Pso at the IC_{50} value specific to the cell type. Cells were monitored for 10 days, and colonies were stained with crystal violet and counted manually. Data are expressed as mean ± s.e.m. of three independent experiments. (**C**) A mammosphere assay was performed using 4×10^3 cells (ALDH$^-$ and ALDH$^+$ cells) on ultra-low attachment plates. Cells were treated with IC_{50} dose of Pso and allowed to grow for 2 weeks followed by counting of mammospheres. Data are expressed as mean ± s.e.m. of two independent experiments. (**D**) To assess apoptosis induced by Pso, ALDH$^-$ cells, ALDH$^+$ cells, and commercial BCSCs were treated with Pso for 24 h. Cells were stained with FITC-Annexin-V and propidium iodide and analyzed by flow cytometery. Data are expressed as mean ± s.e.m. of three independent experiments. Student's *t*-test was used to calculate statistical significance. *$P<0.05$, **$P<0.005$, and ***$P<0.0001$. The full colour version of this figure is available at *British Journal of Cancer* online.

ALDH$^+$ cells as compared with that in the scrambled siRNA-transfected cells (Figure 6C). Furthermore, western blot analysis confirmed decreased levels of NOTCH1 and its downstream target, HRT-1 expression in siNOTCH1-transfected cells compared with the scrambled siRNA-transfected cells (Figure 6D). Further, a significant decrease in the expression of β-catenin and the mesenchymal marker vimentin were observed in NOTCH1-silenced ALDH$^-$ and ALDH$^+$ cells. In addition, we also examined additional EMT markers, Slug and twist (data not shown), and all of these were downregulated in siNOTCH1-transfected ALDH$^-$ and ALDH$^+$ cells compared with control cells (Figure 6D). These results suggest that NOTCH1 may be an important target for inhibiting BCSC growth.

DISCUSSION

A critical role for cancer stem cells in initiation, progression, and metastasis has been well established in many cancer types including BC (Croker and Allan, 2008; Alison *et al*, 2012). Breast cancer stem cells were initially characterized on the basis of cell surface markers such as CD44^{hi} and CD24^{loW} in breast tumours, but, recent studies indicate that ALDH1 may be a better marker for BCSCs due to the high tumourigenicity of cells that express high levels of ALDH1 (Ginestier *et al*, 2007). Additional clinical evidence suggests a correlation between ALDH expression and tumour grade (Charafe-Jauffret *et al*, 2010; Resetkova *et al*, 2010; Marcato *et al*, 2011b; Tsang *et al*, 2012). Hence, we used ALDH$^+$ as a marker for our experiments. In our studies, ALDH$^+$ cells exhibited an aggressive phenotype with higher cell proliferation, potent colony-forming ability, more mammosphere formation, and a high potency to invade and migrate compared to ALDH$^-$ cells. More specifically, ALDH$^+$ cells showed a significant increase in colony formation (five-fold higher) and mammosphere formation (2.5-fold) than ALDH$^-$ cells, supporting the notion that BCSCs may be responsible for the chemoresistance of BCCs. BSCSs have, in fact, been shown previously to cause chemoresistance and to be responsible for tumour regrowth (Velasco-Velazquez *et al*, 2012; Zhang *et al*, 2012). Similarly, our studies indicated that known chemotherapeutic agents such as doxorubicin, docetaxel, and 5-FU fail to sensitize ALDH$^+$ cells; however, significant growth arrest was observed in ALDH$^-$ cells in response to these agents. Similar results were observed with commercially available BCSC cells. A recent study showed that either epirubicin or paclitaxel-based chemotherapy enriches ALDH$^+$ cells, which causes resistance to these drugs (Tanei *et al*, 2009). The reasons for chemoresistance of BCSCs may be explained by the expression of higher levels of ABC transporters, which efflux the drugs (Patrawala *et al*, 2005) and/or by the function of the ALDH enzyme to detoxify the drugs (Croker and Allan, 2012). Hence, it is important to identify new therapeutic agents to target the molecular signaling pathways of BCSCs origin, self-renewal, maintenance, and their niche as well as to target the pathways that confer these cells with resistance to current chemotherapies.

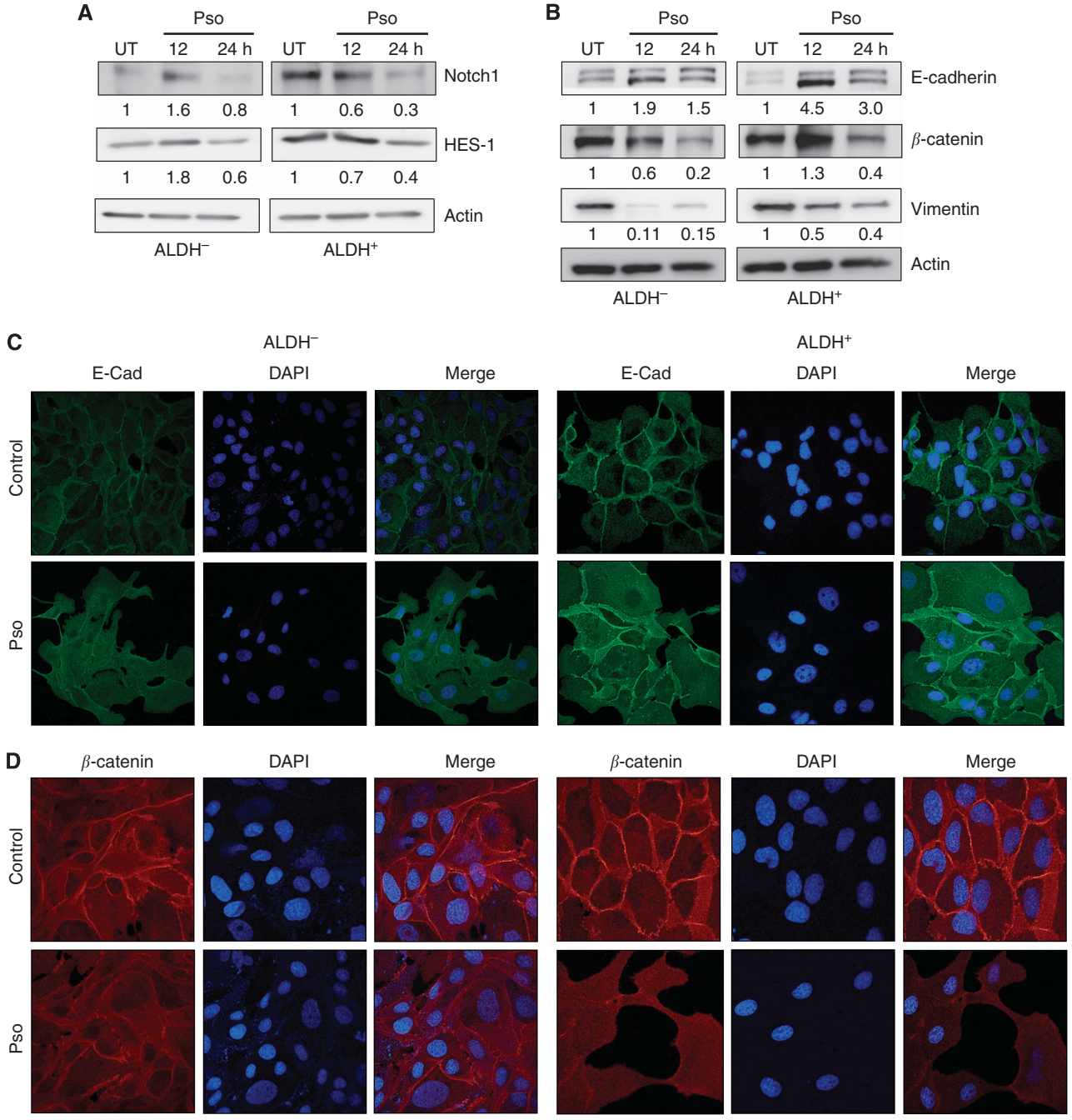

Figure 4. Psoralidin inhibits NOTCH1 signaling and EMT in ALDH$^-$ and ALDH$^+$ cells. (**A**) ALDH$^-$ and ALDH$^+$ cells were treated with vehicle or the IC_{50} dose of Pso. Total cell lysates were prepared, and equal amounts of protein were subjected to western blot analysis for NOTCH1, HES1, and actin proteins. (**B**) Total protein lysates were utilized for western blot analysis to determine the expression of the EMT markers E-cadherin, β-catenin, and vimentin. Actin was used as a loading control. (**C**) E-cadherin, and (**D**) β-catenin expression and localization were visualized by confocal microscopy in vehicle- and Pso-treated ALDH$^-$ and ALDH$^+$ cells.

In the present study, we elucidated the anticancer potency of Pso, a naturally occurring furanocoumarin that possesses anticancer properties (Das *et al*, 2013). Although, we expected that BCSCs may be more resistant to Pso, the difference between the IC_{50} value for ALDH$^-$ cells and that for ALDH$^+$ cells or the commercial BCSCs was small, suggesting that Pso is a putative agent for the specific targeting of cancer cells (BCCs or BCSCs). In addition to cell viability, Pso also inhibited colony and mammosphere formation in both BCCs and BCSCs. Previous reports suggested that ALDH$^+$ cells upregulate stem cell-associated genes (Charafe-Jauffret *et al*, 2009), aiding mammosphere formation. More importantly, activation of AKT increases mammosphere formation in BCCs (Korkaya *et al*, 2009). On the other hand, silencing of NOTCH1 expression significantly reduced the number and size of mammospheres (Mao *et al*, 2013). In this study, we also found that Pso not only inhibited mammosphere formation but also drastically reduced the size of the mammospheres. Chemotherapeutic agents such as paclitaxel fail to effectively suppress the mammosphere-forming ability (Mao *et al*, 2013) in cell culture models. To confirm the effects of Pso, we grew mammospheres in medium with and without serum as BCSCs can form mammospheres in the absence of serum. ALDH$^+$ cells grown under both conditions formed a significant number of mammospheres compared with ALDH$^-$ cells, and Pso effectively suppressed mammosphere formation under both conditions (data not shown).

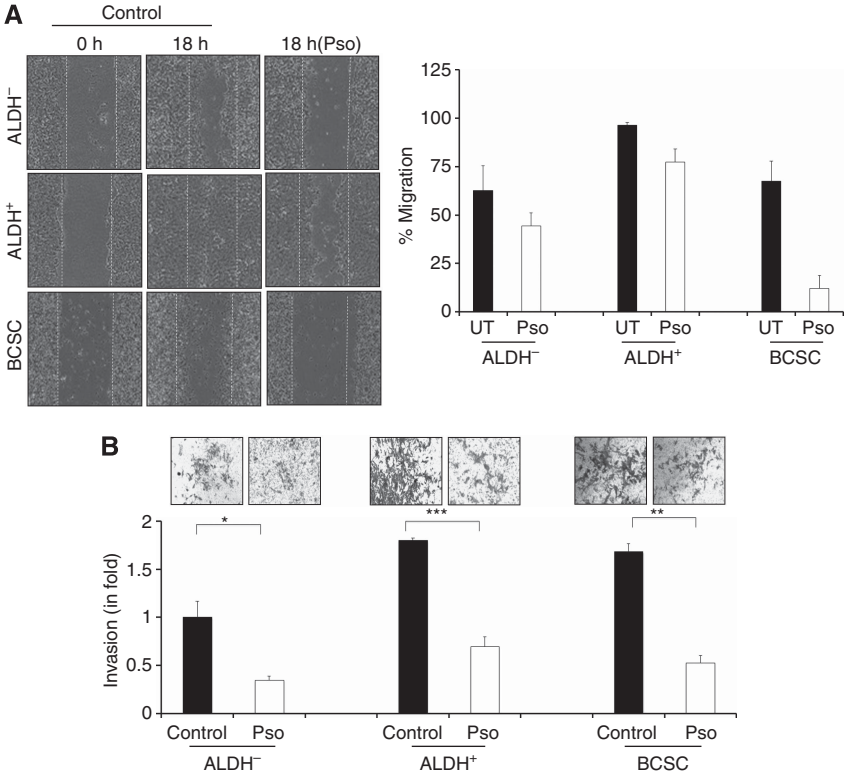

Figure 5. Psoralidin inhibits migration and invasion in BCCs and BCSCs. (**A**) ALDH$^-$ cells, ALDH$^+$ cells, and commercial BCSCs were plated in six-well plates and grown until confluent. A uniform wound was created in the center of the monolayer. The wound gap was photographed in a Biostation CT programmed to take pictures every 2 h. The distance between the edges of wound was measured in μM using NIS-Element software, and statistical analysis was performed. Data are expressed as mean ± s.e.m. of two independent experiments. (**B**) A transwell invasion assay was performed with ALDH$^-$ cells, ALDH$^+$ cells, and commercial BCSCs using Boyden chambers. The cells were treated with vehicle or the IC_{50} dose of Pso and allowed to migrate towards the lower chamber. The invasive cells were stained with crystal violet and counted. Data are expressed as mean ± s.e.m. of three independent experiments. Student's *t*-test was used to calculate statistical significance. *$P<0.05$, **$P<0.005$, and ***$P<0.0001$.

Several pathways have been implicated in the regulation of BCSC self-renewal. Among these pathways, NOTCH signaling is associated with the regulation of cell fate at several distinct developmental stages of the mammary gland and its deregulation has been implicated in cancer initiation, cancer progression, and BCC survival (Dontu *et al*, 2004; Shi and Harris, 2006; Al-Hussaini *et al*, 2011). Higher expression of NOTCH1 in BCSCs is associated with chemoresistance and radioresistance (Velasco-Velazquez *et al*, 2012). Studies have shown that inhibition of NOTCH1 sensitizes BCCs to paclitaxel (Mao *et al*, 2013), doxorubicin, and docetaxel-induced apoptosis (Zang *et al*, 2010). In our studies, Pso inhibited NOTCH1 activation in both ALDH$^-$ and ALDH$^+$ cells. To determine whether NOTCH1 is responsible for the inhibition of growth and EMT, we silenced NOTCH1 with siRNA and obtained similar results, revealing that NOTCH1 is an important player in the Pso-induced anticancer effects in BSCSs.

NOTCH1 is considered an important therapeutic target for CSCs, and in this vein, a number of NOTCH1 inhibitors are being developed (Al-Hussaini *et al*, 2011). Most of the inhibitors are currently in preclinical investigations. For example, the γ-secretase inhibitors (GSI) have shown some promising potential; however, these inhibitors also exhibit toxicity (Pannuti *et al*, 2010). Several dietary agents are reported to target NOTCH signaling as well. For example, genistein from soy products inhibited NOTCH signaling and resulted in induction of apoptosis in pancreatic (Wang *et al*, 2006) and prostate cancer cells (Wang *et al*, 2011). Sulforaphane, a major ingredient from cruciferous vegetables, has been shown to inhibit NOTCH signaling in BCSCs and result in tumour regression in *in vivo* models. Similarly, querctein, curcumin, and resveratrol also have been shown to inhibit NOTCH expression in different cancer types and result in growth arrest (Espinoza and Miele, 2013).

The NOTCH pathway is frequently over activated in BC and is related to the development and maintenance of BCSCs possibly via the initiation of EMT-like processes (Pannuti *et al*, 2010; Lombardo *et al*, 2012; Smalley *et al*, 2012). Thus, NOTCH has received increased attention as a target to eliminate BCSCs (Ponti *et al*, 2005). These cells were shown to exhibit more aggressive phenotypes and at the molecular level, these phenotypes are regulated by transcription factors, such as Twist, Snail, or Zeb (Lehmann *et al*, 2012). Loss of E-cadherin and upregulation of β-catenin expression is a classical molecular switch for EMT, which initiates the loss of apical polarity by altering cytoskeleton organisation and leads to spindle-shaped morphologic features (Leong *et al*, 2007; Gangopadhyay *et al*, 2013). In our studies, induction of E-cadherin and inhibition of β-catenin expression in Pso-treated BCSCs and BCCs suggest that the EMT phenomenon was completely abolished by Pso. Furthermore, immunofluorescence analysis confirmed that E-cadherin is significantly upregulated in the cell membrane and cellular junctions, and simultaneous inhibition of β-catenin expression suggested that Pso may be a potent compound to inhibit EMT in BCCs. Moreover, the inhibition of invasion and migration by Pso in ALDH$^-$ and ALDH$^+$ cells was strongly correlated with molecular changes in EMT markers.

Nuclear factor κB, a known pro-survival transcription factor, governs cell survival and proliferation, and recent studies suggest that activation of the NFκB signaling pathway is involved in EMT induction in cultured cells and *in vivo* (Thiery *et al*, 2009). Furthermore, activation of NFκB is a key regulator of BCSCs

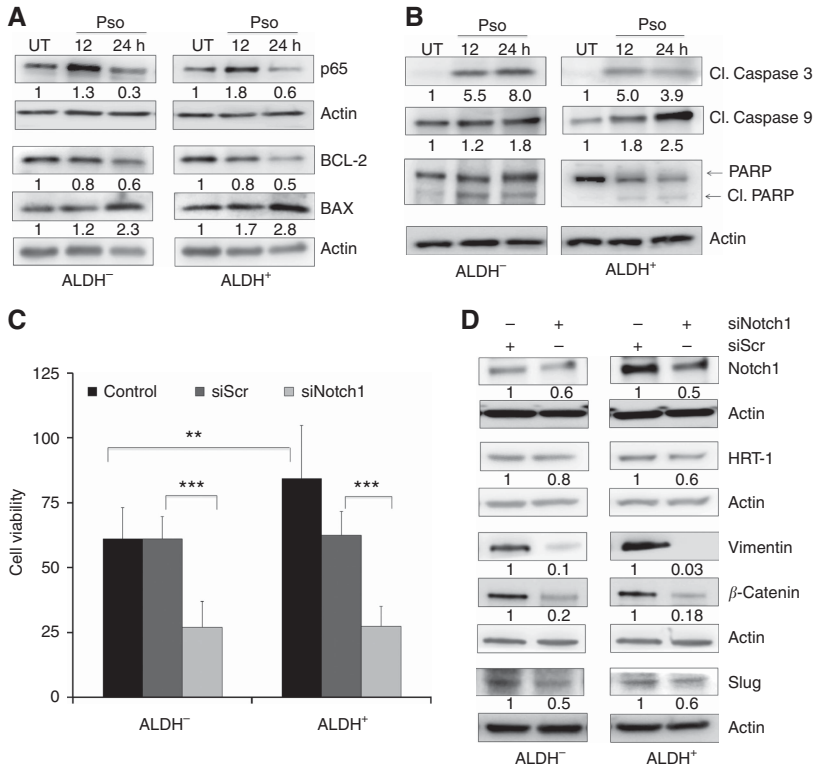

Figure 6. Psoralidin inhibits pro-survival genes and activates the pro-apoptotic cascade in ALDH$^-$ and ALDH$^+$ cells. (**A**) ALDH$^-$ and ALDH$^+$ cells were treated with vehicle or an IC_{50} dose of Pso. Total cell lysates were prepared and equal amounts of proteins were subjected to western blot analysis to examine the expression pattern of p65, BAX, and BCL-2. (**B**) Total cell lysates were subjected to western blot analysis for caspase-3, caspase-9, and PARP. Actin was used as a loading control. (**C**) ALDH$^-$ and ALDH$^+$ cells were plated in six-well plates. Cells were transiently transfected with scrambled (Scr) or NOTCH1 siRNA (siNOTCH1) for 36 h. Cells were harvested, and cell proliferation was measured. (**D**) Whole-cell lysates were prepared and utilized for western blot analysis for NOTCH1, HRT-1, vimentin, β-catenin, and Slug. Actin was used as a loading control. Data are expressed as mean ± s.e.m. of two independent experiments. Student's *t*-test was used to calculate statistical significance. $^{**}P<0.005$ and $^{***}P<0.0001$.

(Liu *et al*, 2010). Psoralidin inhibited p65 expression as well as the expression of the downstream target BCL-2 in BCSCs. A recent study reported that knock down of NOTCH1 induces BCC apoptosis through the inactivation of NFκB, suggesting crosstalk between NOTCH1 and NFκB activation, and silencing of NOTCH1 resulted in downregulation of NFκB in BCSCs (Mao *et al*, 2013) and growth arrest in leukemic cells (Vilimas *et al*, 2007). Downregulation of NOTCH1 and NFκB activation in ALDH$^-$ and ALDH$^+$ cells by Pso implicates activation of pro-apoptotic signaling in the function of BCSCs. In addition, induction of Bax and a concomitant increase in caspase signaling (caspase-9 and -3) followed by cleaved PARP led to cell death in BCSC cells.

Breast cancer stem cells are resistant to current chemotherapeutic regimens and may be responsible for EMT and metastasis in BC patients. Psoralidin, a natural compound found in the seeds of the Asian medicinal plant *Psoralea corylifolia*, effectively downregulated NOTCH1 signaling, which resulted in the downregulation of EMT and growth arrest in BCSCs. Inhibition of pro-survival signaling and simultaneous induction of the pro-apoptotic machinery appears to be a novel strategy for the eradication of BCSCs; however, additional studies are required to confirm the anticancer role of Pso in animal models.

CONFLICT OF INTEREST

The authors declare no conflict of interest.

REFERENCES

Al-Hajj M, Wicha MS, Benito-Hernandez A, Morrison SJ, Clarke MF (2003) Prospective identification of tumorigenic breast cancer cells. *Proc Natl Acad Sci USA* **100**(7): 3983–3988.

Al-Hussaini H, Subramanyam D, Reedijk M, Sridhar SS (2011) Notch signaling pathway as a therapeutic target in breast cancer. *Mol Cancer Ther* **10**(1): 9–15.

Alison MR, Lin WR, Lim SM, Nicholson LJ (2012) Cancer stem cells: in the line of fire. *Cancer Treat Rev* **38**(6): 589–598.

Andersen P, Uosaki H, Shenje LT, Kwon C (2012) Non-canonical Notch signaling: emerging role and mechanism. *Trends Cell Biol* **22**(5): 257–265.

Charafe-Jauffret E, Ginestier C, Iovino F, Tarpin C, Diebel M, Esterni B, Houvenaeghel G, Extra JM, Bertucci F, Jacquemier J, Xerri L, Dontu G, Stassi G, Xiao Y, Barsky SH, Birnbaum D, Viens P, Wicha MS (2010) Aldehyde dehydrogenase 1-positive cancer stem cells mediate metastasis and poor clinical outcome in inflammatory breast cancer. *Clin Cancer Res* **16**(1): 45–55.

Charafe-Jauffret E, Ginestier C, Iovino F, Wicinski J, Cervera N, Finetti P, Hur MH, Diebel ME, Monville F, Dutcher J, Brown M, Viens P, Xerri L, Bertucci F, Stassi G, Dontu G, Birnbaum D, Wicha MS (2009) Breast cancer cell lines contain functional cancer stem cells with metastatic capacity and a distinct molecular signature. *Cancer Res* **69**(4): 1302–1313.

Croker AK, Allan AL (2008) Cancer stem cells: implications for the progression and treatment of metastatic disease. *J Cell Mol Med* **12**(2): 374–390.

Croker AK, Allan AL (2012) Inhibition of aldehyde dehydrogenase (ALDH) activity reduces chemotherapy and radiation resistance of stem-like ALDHhiCD44(+) human breast cancer cells. *Breast Cancer Res Treat* **133**(1): 75–87.

Das TP, Suman S, Damodaran C (2013) Reactive oxygen species generation inhibits epithelial-mesenchymal transition and promotes growth arrest in prostate cancer cells. *Mol Carcinog;* e-pub ahead print 8 March 2013; doi:10.1002/mc.22014.

Dontu G, Jackson KW, McNicholas E, Kawamura MJ, Abdallah WM, Wicha MS (2004) Role of Notch signaling in cell-fate determination of human mammary stem/progenitor cells. *Breast Cancer Res* **6**(6): R605–R615.

Espinoza I, Miele L (2013) Notch inhibitors for cancer treatment. *Pharmacol Ther* **139**(2): 95–110.

Gangopadhyay S, Nandy A, Hor P, Mukhopadhyay A (2013) Breast cancer stem cells: a novel therapeutic target. *Clin Breast Cancer* **13**(1): 7–15.

Ginestier C, Hur MH, Charafe-Jauffret E, Monville F, Dutcher J, Brown M, Jacquemier J, Viens P, Kleer CG, Liu S, Schott A, Hayes D, Birnbaum D, Wicha MS, Dontu G (2007) ALDH1 is a marker of normal and malignant human mammary stem cells and a predictor of poor clinical outcome. *Cell Stem Cell* **1**(5): 555–567.

Giordano A, Gao H, Anfossi S, Cohen E, Mego M, Lee BN, Tin S, De Laurentiis M, Parker CA, Alvarez RH, Valero V, Ueno NT, De Placido S, Mani SA, Esteva FJ, Cristofanilli M, Reuben JM (2012) Epithelial-mesenchymal transition and stem cell markers in patients with HER2-positive metastatic breast cancer. *Mol Cancer Ther* **11**(11): 2526–2534.

Grimshaw MJ, Cooper L, Papazisis K, Coleman JA, Bohnenkamp HR, Chiapero-Stanke L, Taylor-Papadimitriou J, Burchell JM (2008) Mammosphere culture of metastatic breast cancer cells enriches for tumorigenic breast cancer cells. *Breast Cancer Res* **10**(3): R52.

Grudzien P, Lo S, Albain KS, Robinson P, Rajan P, Strack PR, Golde TE, Miele L, Foreman KE (2010) Inhibition of Notch signaling reduces the stem-like population of breast cancer cells and prevents mammosphere formation. *Anticancer Res* **30**(10): 3853–3867.

Gulappa T, Reddy RS, Suman S, Nyakeriga AM, Damodaran C (2013) Molecular interplay between cdk4 and p21 dictates G/G cell cycle arrest in prostate cancer cells. *Cancer Lett* **337**(2): 177–183.

Iso T, Kedes L, Hamamori Y (2003) HES and HERP families: multiple effectors of the Notch signaling pathway. *J Cell Physiol* **194**(3): 237–255.

Korkaya H, Paulson A, Charafe-Jauffret E, Ginestier C, Brown M, Dutcher J, Clouthier SG, Wicha MS (2009) Regulation of mammary stem/progenitor cells by PTEN/Akt/beta-catenin signaling. *PLoS Biol* **7**(6): e1000121.

Lehmann C, Jobs G, Thomas M, Burtscher H, Kubbies M (2012) Established breast cancer stem cell markers do not correlate with in vivo tumorigenicity of tumor-initiating cells. *Int J Oncol* **41**(6): 1932–1942.

Leong KG, Niessen K, Kulic I, Raouf A, Eaves C, Pollet I, Karsan A (2007) Jagged1-mediated Notch activation induces epithelial-to-mesenchymal transition through Slug-induced repression of E-cadherin. *J Exp Med* **204**(12): 2935–2948.

Liu M, Sakamaki T, Casimiro MC, Willmarth NE, Quong AA, Ju X, Ojeifo J, Jiao X, Yeow WS, Katiyar S, Shirley LA, Joyce D, Lisanti MP, Albanese C, Pestell RG (2010) The canonical NF-kappaB pathway governs mammary tumorigenesis in transgenic mice and tumor stem cell expansion. *Cancer Res* **70**(24): 10464–10473.

Lombardo Y, Filipovic A, Molyneux G, Periyasamy M, Giamas G, Hu Y, Trivedi PS, Wang J, Yague E, Michel L, Coombes RC (2012) Nicastrin regulates breast cancer stem cell properties and tumor growth in vitro and in vivo. *Proc Natl Acad Sci USA* **109**(41): 16558–16563.

Mao J, Song B, Shi Y, Wang B, Fan S, Yu X, Tang J, Li L (2013) ShRNA targeting Notch1 sensitizes breast cancer stem cell to paclitaxel. *Int J Biochem Cell Biol* **45**(6): 1064–1073.

Marcato P, Dean CA, Giacomantonio CA, Lee PW (2011a) Aldehyde dehydrogenase: its role as a cancer stem cell marker comes down to the specific isoform. *Cell Cycle* **10**(9): 1378–1384.

Marcato P, Dean CA, Pan D, Araslanova R, Gillis M, Joshi M, Helyer L, Pan L, Leidal A, Gujar S, Giacomantonio CA, Lee PW (2011b) Aldehyde dehydrogenase activity of breast cancer stem cells is primarily due to isoform ALDH1A3 and its expression is predictive of metastasis. *Stem Cells* **29**(1): 32–45.

Miele L (2006) Notch signaling. *Clin Cancer Res* **12**(4): 1074–1079.

Pannuti A, Foreman K, Rizzo P, Osipo C, Golde T, Osborne B, Miele L (2010) Targeting Notch to target cancer stem cells. *Clin Cancer Res* **16**(12): 3141–3152.

Patrawala L, Calhoun T, Schneider-Broussard R, Zhou J, Claypool K, Tang DG (2005) Side population is enriched in tumorigenic, stem-like cancer cells, whereas ABCG2+ and ABCG2- cancer cells are similarly tumorigenic. *Cancer Res* **65**(14): 6207–6219.

Ponti D, Costa A, Zaffaroni N, Pratesi G, Petrangolini G, Coradini D, Pilotti S, Pierotti MA, Daidone MG (2005) Isolation and in vitro propagation of tumorigenic breast cancer cells with stem/progenitor cell properties. *Cancer Res* **65**(13): 5506–5511.

Resetkova E, Reis-Filho JS, Jain RK, Mehta R, Thorat MA, Nakshatri H, Badve S (2010) Prognostic impact of ALDH1 in breast cancer: a story of stem cells and tumor microenvironment. *Breast Cancer Res Treat* **123**(1): 97–108.

Shi W, Harris AL (2006) Notch signaling in breast cancer and tumor angiogenesis: cross-talk and therapeutic potentials. *J Mammary Gland Biol Neoplasia* **11**(1): 41–52.

Smalley M, Piggott L, Clarkson R (2012) Breast cancer stem cells: obstacles to therapy. *Cancer Lett* **338**(1): 57–62.

Srinivasan S, Koduru S, Kumar R, Venguswamy G, Kyprianou N, Damodaran C (2009) Diosgenin targets Akt-mediated prosurvival signaling in human breast cancer cells. *Int J Cancer* **125**(4): 961–967.

Srinivasan S, Ranga RS, Burikhanov R, Han SS, Chendil D (2007) Par-4-dependent apoptosis by the dietary compound withaferin A in prostate cancer cells. *Cancer Res* **67**(1): 246–253.

Stockler M, Wilcken NR, Ghersi D, Simes RJ (2000) Systematic reviews of chemotherapy and endocrine therapy in metastatic breast cancer. *Cancer Treat Rev* **26**(3): 151–168.

Suman S, Kurisetty KV, Das TP, Vadodkar V, Ramos G, Lakshmanaswamy R, Damodaran C (2013) Activation of AKT signaling promotes Epithelial-Mesenchymal Transition and tumor growth in colorectal cancer cells. *MolCarcino*. e-pub ahead of print 2 September 2013; doi:10.1002/mc.22076.

Tanei T, Morimoto K, Shimazu K, Kim SJ, Tanji Y, Taguchi T, Tamaki Y, Noguchi S (2009) Association of breast cancer stem cells identified by aldehyde dehydrogenase 1 expression with resistance to sequential Paclitaxel and epirubicin-based chemotherapy for breast cancers. *Clin Cancer Res* **15**(12): 4234–4241.

Thiery JP, Acloque H, Huang RY, Nieto MA (2009) Epithelial-mesenchymal transitions in development and disease. *Cell* **139**(5): 871–890.

Tsang JY, Huang YH, Luo MH, Ni YB, Chan SK, Lui PC, Yu AM, Tan PH, Tse GM (2012) Cancer stem cell markers are associated with adverse biomarker profiles and molecular subtypes of breast cancer. *Breast Cancer Res Treat* **136**(2): 407–417.

Vadodkar AS, Suman S, Lakshmanaswamy R, Damodaran C (2012) Chemoprevention of breast cancer by dietary compounds. *Anticancer Agents Med Chem* **12**(10): 1185–1202.

Velasco-Velazquez MA, Homsi N, De La Fuente M, Pestell RG (2012) Breast cancer stem cells. *Int J Biochem Cell Biol* **44**(4): 573–577.

Velasco-Velazquez MA, Popov VM, Lisanti MP, Pestell RG (2011) The role of breast cancer stem cells in metastasis and therapeutic implications. *Am J Pathol* **179**(1): 2–11.

Vilimas T, Mascarenhas J, Palomero T, Mandal M, Buonamici S, Meng F, Thompson B, Spaulding C, Macaroun S, Alegre ML, Kee BL, Ferrando A, Miele L, Aifantis I (2007) Targeting the NF-kappaB signaling pathway in Notch1-induced T-cell leukemia. *Nat Med* **13**(1): 70–77.

Visvader JE, Lindeman GJ (2008) Cancer stem cells in solid tumours: accumulating evidence and unresolved questions. *Nat Rev Cancer* **8**(10): 755–768.

Wang Z, Li Y, Ahmad A, Banerjee S, Azmi AS, Kong D, Wojewoda C, Miele L, Sarkar FH (2011) Down-regulation of Notch-1 is associated with Akt and FoxM1 in inducing cell growth inhibition and apoptosis in prostate cancer cells. *J Cell Biochem* **112**(1): 78–88.

Wang Z, Zhang Y, Banerjee S, Li Y, Sarkar FH (2006) Inhibition of nuclear factor kappab activity by genistein is mediated via Notch-1 signaling pathway in pancreatic cancer cells. *Int J Cancer* **118**(8): 1930–1936.

Yoshioka T, Umekita Y, Ohi Y, Souda M, Sagara Y, Sagara Y, Sagara Y, Rai Y, Tanimoto A (2011) Aldehyde dehydrogenase 1 expression is a predictor of poor prognosis in node-positive breast cancers: a long-term follow-up study. *Histopathology* **58**(4): 608–616.

Zang S, Chen F, Dai J, Guo D, Tse W, Qu X, Ma D, Ji C (2010) RNAi-mediated knockdown of Notch-1 leads to cell growth inhibition and enhanced chemosensitivity in human breast cancer. *Oncol Rep* **23**(4): 893–899.

Zhang X, Zhang S, Liu Y, Liu J, Ma Y, Zhu Y, Zhang J (2012) Effects of the combination of RAD001 and docetaxel on breast cancer stem cells. *Eur J Cancer* **48**(10): 1581–1592.